A&A 418, 225–233 (2004)
DOI: 10.1051/0004-6361:20040023
© ESO 2004

Astronomy & Astrophysics

Blue loops of intermediate mass stars

II. Metallicity and blue loops

H. Y. Xu[1] and Y. Li[1,2]

[1] National Astronomical Observatories/Yunnan Observatory, PO Box 110, 650011 Kunming, PR China
[2] Joint Laboratory for Optical Astronomy, Chinese Academy of Sciences, PR China

Received 12 May 2003 / Accepted 19 December 2003

Abstract. Based on the results of the blue loop formation for models of solar-like metallicity, we have explored the blue loop evolution of metal-poor stars. Three series of models with a wide range of metallicity and the initial helium abundance were calculated. An important parameter, η_c, defined as the envelope convection mass divided by the total envelope mass at the bottom of the RGB, was introduced as a criterion to determine the formation of the blue loop. We have found that the low-Z models will develop extensive blue loops when η_c is lower than a critical value η_{crit}. The physical explanation for this result could be as follows. Lower Z reduces the envelope opacity and leads to a hotter stellar envelope and a bluer RGB. Thus the model will have a smaller η_a at the top and an even smaller η_c at the bottom of the RGB. When η_c is lower than the critical value η_{crit}, the envelope is radiation-dominated. Under this condition and the constraint of the virial theorem, the response of the star to the increase of the stellar luminosity is to contract to increase the thermal conductivity coefficient in the stellar envelope and to form a blue loop. Compared with the high-Z models, we have confirmed that the development of convection in the stellar envelope is a crucial factor to determine the formation of the blue loop, but the low-Z models reach low η_c values in a different way from the high-Z models, in which the modulation of the nuclear reaction rates by higher ^{14}N abundance in the H-burning shell is responsible for the stars to get small η_c values. It has been found that η_{crit} depends not only on the stellar mass, but also on metallicity and the initial helium abundance. Our numerical results show that η_{crit} decreases with Z while slowly increases with Y.

Key words. stars: evolution – stars: interiors – stars: Hertzsprung-Russell (HR) and C-M diagrams

1. Introduction

The formation and extension of the blue loop is closely related to many physical conditions in the evolution of intermediate mass stars. In a previous paper (Xu & Li 2004, hereafter referred to as Paper I), we have made extensive investigations on the formation of the blue loop for stellar models of solar-like composition. We found that the blue loop evolution depends closely on the development of the envelope convection and nuclear energy production in the H-burning shell. Here we will pay more attention to models with different metallicity, especially those metal-poor models that develop very extended blue loops.

Chemical composition is of strong effects on the formation and extension of the blue loop. There is a general tendency that higher helium abundance with constant metallicity leads to more extended blue loops (Robertson 1971; Robertson 1972b; Fricke & Strittmatter 1972). However, the relationship between the blue loop and the metallicity is more complicated. Previous investigations based on the stellar models of different Z suggested that lower metallicity made more extended blue loop (Hallgren & Cox 1970; Robertson 1971; Robertson 1972b; Castellani et al. 1990; Alongi et al. 1991; Schaller et al. 1992; Pols et al. 1998). Due to the variation of the initial X, Y, and Z in most of the models and the incomplete coverage of Z values, the detailed relationship of the blue loop to the metallicity cannot be found clearly and straightforwardly from the literature. Two sequences of models with $Y = 0.27$ in Bono et al. (2000, hereafter BY27) and with $X = 0.70$ in Alcock & Paczynski (1978, hereafter AX70) are helpful for understanding the dependance of the blue loop on Z, because they have adequate coverage of Z values. Although the two sequences used different opacity tables and other input physics, they showed a similar trend of the blue loop evolution, i.e., when the stellar mass is higher than about 5 $M_\odot$, the extension of the blue loop decreases as Z increases from 0.004 to 0.01, and increases as Z increases from 0.01 to 0.02, while when the stellar mass is lower than 5 $M_\odot$, the extension of the blue loop decreases monotonically as Z increases from 0.004 to 0.02. Dominguez's (1999) models share similar properties of the blue loop evolution but their choice of Y or X is not constant when Z varies. Early attempts made to determine the effect of composition on the blue loop showed also other different views (Hofmeister 1967; Schlesinger 1969; Hallgren & Cox 1970; Harris & Deupree 1976).

Send offprint requests to: H. Y. Xu, e-mail: xuhuayin@sohu.com

Article published by EDP Sciences and available at http://www.aanda.org or http://dx.doi.org/10.1051/0004-6361:20040023

The physical relationship between the metallicity and the blue loop has not been clearly understood up to now. The location of the hydrogen profile outside the helium core was sometimes considered as a possible factor (Robertson 1972a; Stothers & Chin 1968, 1973; Schlesinger 1977; Stothers & Chin 1991). Another possible factor was lower opacity due to lower metallicity, since lower opacity in the radiative envelope could make a star bluer (Stothers & Chin 1968, 1973; Schlesinger 1977).

Series of evolution models with different Z but constant X or Y are rare in the literature, but they are desirable for the investigation of the relationship between the metallicity and the blue loop. In this paper, we shall investigate the development of the blue loop under different metallicity, in order to see whether the formation mechanism of the blue loop for high metallicity models differs from that for low metallicity models, and how the metallicity affects the formation of the blue loop.

Physical inputs adopted in our model calculations are similar to those in Paper I and briefly introduced in Sect. 2. Properties of the evolution models are discussed in Sect. 3. Comparisons of the evolution models with different metallicity are given in Sect. 4. Furthermore, we investigate the structure of the stellar models during the blue loop phase and discuss the formation mechanism of the blue loop in Sect. 5. Conclusions and discussions are summarized in Sect. 6.

2. Physical assumptions and computation methods

Physical assumptions and computation methods adopted in the present investigation were similar to those in Paper I, and here we only give a brief summary.

The rates of the nuclear reactions were taken from Caughlan & Fowler (1988). The OPAL opacities G91hz series (Iglesias & Rogers 1996) were used in the high temperature region and the low temperature opacities were taken from Alexander & Ferguson (1994). Energy transfer by convection was treated according to the standard mixing-length theory and the boundaries of the convection zones were determined by the Schwarzschild criterion (Cox & Giuli 1968; Huang & Yu 1998). The ratio of the mixing-length to local pressure scale height, α, was chosen to be 1.8. Overshooting and mass loss were ignored. Our revised stellar evolution code was originally described by Kippenhahn et al. (1967).

Models with the metal abundance of $Z = 0.020$, 0.018, 0.016, ... , 0.004 and the helium abundance of $Y = 0.28$, 0.26, 0.23 were calculated. For the considered heavy element abundance, we chose $X_{\rm N} = 0.228Z$ as the initial nitrogen abundance, which was the sum of the original abundance of ^{14}N and ^{12}C, and $X_{\rm O} = 0.502Z$ as the initial oxygen abundance. These choices of the initial abundance were referred to a solar-scaled heavy element distribution (Anders & Grevesse 1989; Grevesse & Noels 1993).

CN models and CNO models were described in Paper I. The CN models only considered the CN cycle in the hydrogen burning process, and the CNO models were based on an approximation of the CNO bi-cycle (Clayton 1968) and could reproduce most of the properties of stellar models using the nuclear-reaction network. All of these models consisted of enough mass zones and time steps to avoid the numerical inaccuracy.

3. Properties of evolution models

We calculated three series of evolution tracks of a 7 $M_\odot$ model with the considered values of helium abundance. Both the CN and the CNO models were calculated, and their evolution tracks are shown in Figs. 1 and 2, respectively. The three series of the CN models (see Fig. 1) show a common behavior of the blue loop with different Z, and the lower Z always results in more extended blue loops (Hallgren & Cox 1970; Robertson 1971; Robertson 1972b; Castellani et al. 1990; Alongi et al. 1991; Schaller et al. 1992). However, the CNO models (see Fig. 2) show that the width of the blue loop decreases when Z increases from 0.004 to 0.01, and turns to increase when Z increases from 0.01 to 0.02, which is similar to the trend in BY27 and AX70. We regard this result as the actual relationship between Z and the blue loop, because the CNO models are more accurate than the CN models. Comparing Figs. 1 and 2, we can see that the CN and CNO models develop the blue loops when Z is low enough. Similar results can be found in the literature (e.g. Bono et al. 2000). This implies that the low opacity due to low Z in the stellar envelope may be a chief factor to determine the blue loop evolution (Hallgren & Cox 1970; Robertson 1971; Robertson 1972b; Castellani et al. 1990; Alongi et al. 1991; Schaller et al. 1992; Pols et al. 1998). The CNO models develop blue loops again when Z is high enough while the CN models do not. This result indicates that the formation of the blue loop in the low-Z models may be different from that in the high-Z models. The helium abundance has a less but still noticeable effect on the development of the blue loop, and higher Y facilitates in the low Z limit and hampers in the high Z limit the development of the blue loop (Robertson 1971; Robertson 1972b; Fricke & Strittmatter 1972). This result indicates again that the lower opacity due to the higher helium in the low-Z models can affect the blue loop evolution (Schlesinger 1977).

Some critical values during the He-core burning stage are listed in Table 1. An important parameter, η, is defined as the ratio of the envelope convection mass to the total envelope mass (see Paper I):

$$\eta = \frac{M_{\rm con}}{M_{\rm env}}. \quad (1)$$

$\eta_{\rm a}$ and $\eta_{\rm c}$ represent respectively the value of η at the top and the bottom of the red-giant branch (RGB), and $\eta_{\rm min}$ is the smallest value of η when the envelope convection decreases mostly after the ignition of the He core. If there is a blue loop, $\eta_{\rm min}$ will be zero, which means that the envelope is almost wholly in the radiative equilibrium. We mark these points (a, c, and min) in Fig. 3 to clearly indicate their position in the HR diagram (HRD), which is a magnified part of the evolution tracks of the models with $Y = 0.28$ in Fig. 2. Figure 3 shows a typical series of evolution tracks of the CNO models during the early stage of the central He-burning phase, in which the three markers

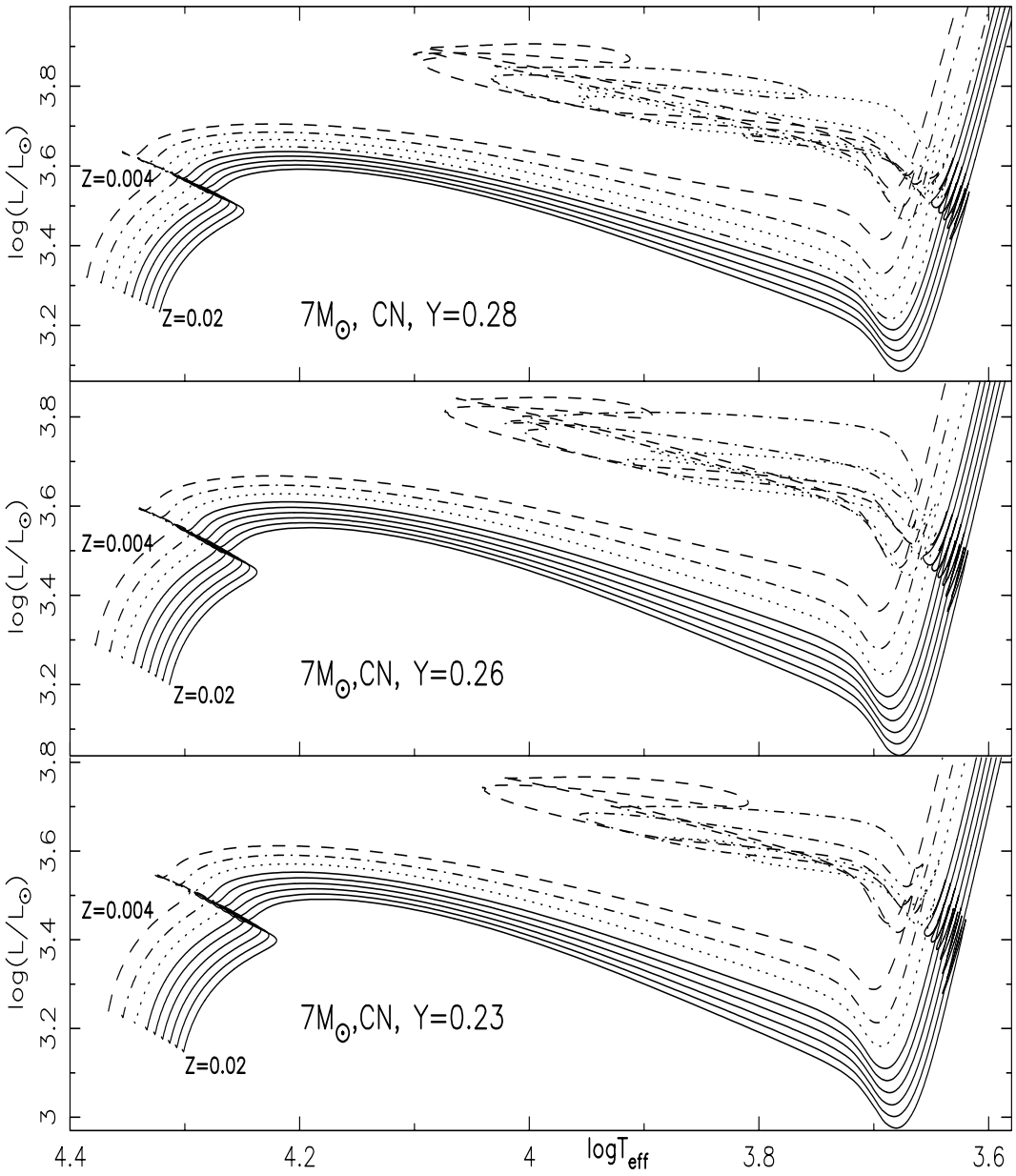

Fig. 1. Evolutionary tracks of the CN models. Models with $Z = 0.004$, 0.006, ..., 0.02 are plotted in each panel, among which the models without the blue loop have solid lines and those having the blue loop have other types of lines.

correspond to the position of η_a (cross), η_c (asterisk) and η_{min} (circle) respectively in the Table 1.

The value of η_a is an important parameter for the formation of the blue loop, which describes how deep the envelope convection can penetrate downward just after the He-core ignition. It can be found from Table 1 and Fig. 3 that a model with a lower Z value gets a smaller η_a value, although its luminosity is higher. The reasons for this effect comes from two aspects. A model with a lower Z value is always brighter than that with a higher Z value in the main sequence and forms a larger He core. At the moment of the central He ignition, the lower Z model has a hotter He core and a hotter envelope. The larger and hotter He core produces a higher luminosity at the top of the RGB, while the hotter envelope makes the energy transfer more efficient and then the underdevelopment of the envelope convection to get a smaller value of η_a. It can be seen in Fig. 3 that a smaller Z leads to a bluer and brighter position a (see the crosses).

It can be found from Table 1 that all the evolution tracks with the blue loops are of comparably low η_c at the bottom of the RGB. This confirms the conclusion in Paper I that a blue loop will be formed if η_c is smaller than a critical value η_{crit}. In the CNO models, η_c increases before about $Z = 0.012$ and then decreases after $Z = 0.012$ when Z increases from 0.004 to 0.02, corresponding to the formation of the blue loops at the high and low Z limit for these series of models. It can be found in the series of $Y = 0.28$ models, however, that a blue loop is formed when $\eta_c = 0.4058$ in the model of $Z = 0.006$, and that there is no blue loop even if $\eta_c = 0.3373$ in the model of $Z = 0.018$. This result indicates that η_{crit} depends not only on

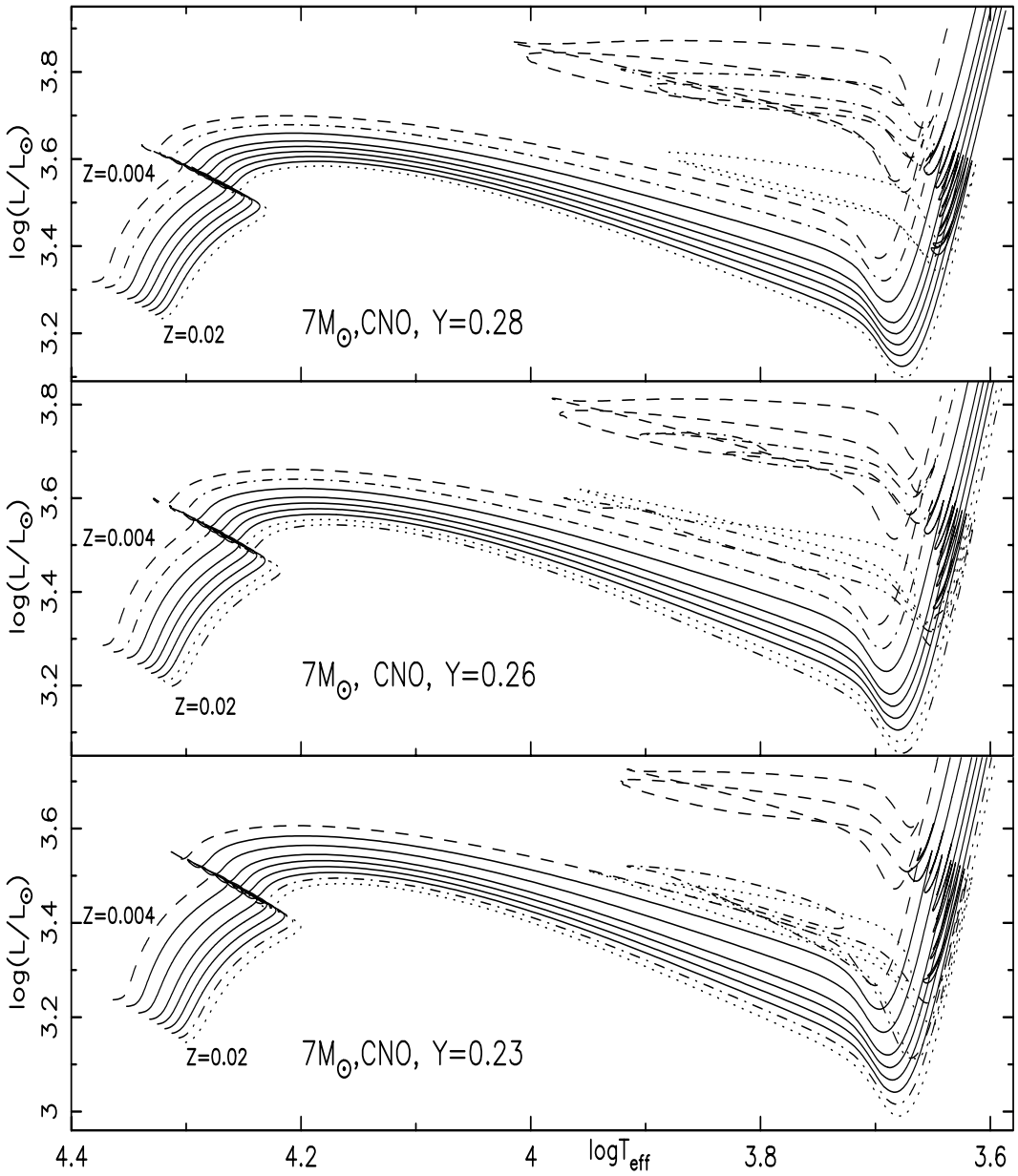

Fig. 2. Evolutionary tracks of the CNO models. Models with Z = 0.004, 0.006, ..., 0.02 are plotted in each panel, among which the models without the blue loop have solid lines and those having the blue loop have other types of lines.

the stellar mass (see Paper I), but also on the metallicity. Low Z reduces the opacity of the stellar envelope, and the critical value of η_c has therefore to vary. From Table 1 it may be approximately concluded that η_{crit} increases as Z decreases, which implies that low-Z models are more available for the formation of the blue loop. Comparing the models with the blue loops at constant Z, we find that η_c increases when Y increases, which implies that η_{crit} increases with Y and that models with higher helium abundance are more suitable for the formation of the blue loop. This result shows the common behavior of the blue loop that higher Y makes more extended blue loops because of lower opacities (Fricke & Strittmatter 1972; Bono et al. 2000).

We find in Fig. 3 that the asterisks are arranged in an arched shape, which is unlike the behavior of the crosses. The distance between each set of the crosses and asterisks is lengthened when Z increases, and the luminosity difference from a to c, $L_a - L_c$ is also enlarged when Z increases. This is the effect of X_N on the RGB evolution as we have discussed in Paper I. It is obvious that a small value of η_c can result in blue loop evolution, but how a star can reach a small η_c may be different between the metal-poor and metal-rich models, and our research will be focused on this question.

On the other hand, the variation of η_{min} in Table 1 shows that the transition from a fairly large η_{min} value (about 0.3) to zero is quite sudden, which strongly indicates that the envelope convection zone is very sensitive to the metallicity and will disappear rapidly as soon as the condition of the formation of the blue loop is satisfied. The circles in Fig. 3 show that the envelope convection becomes the smallest when the star evolves to the bluest tip if there is no blue loop. For those tracks

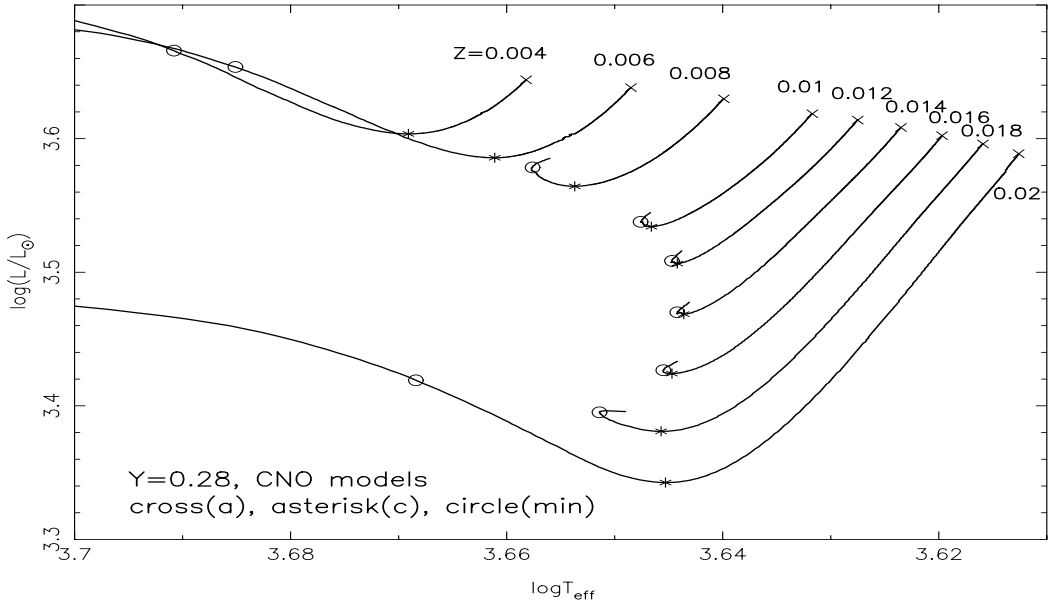

Fig. 3. Evolutionary tracks of the 7 $M_\odot$ stars with $Y = 0.28$, during the early phase of the central He burning. The crosses, asterisks, and circles respectively represent the moment of the top of the RGB (a), the bottom of the RGB (c), and the envelope convection decreases maximally (min).

Table 1. The values of η at the three critical position.

	the CNO Models			the CN Models		
Z	η_a	η_c	η_{min}	η'_a	η'_c	η'_{min}
			$Y = 0.28$			
.020	.9388	.3171	.0000	.9062	.5248	.5157
.018	.9317	.3373	.1993	.8948	.5187	.4978
.016	.9228	.3926	.3636	.8809	.4889	.4573
.014	.9120	.4608	.4349	.8652	.4614	.3960
.012	.8986	.4863	.4627	.8484	.4292	.2983
.010	.8824	.4748	.4324	.8280	.4147	.0000
.008	.8527	.4284	.2878	.7865	.3937	.0000
.006	.8122	.4058	.0000	.7274	.3684	.0000
.004	.7483	.3749	.0000	.6372	.3528	.0000
			$Y = 0.26$			
.020	.9430	.2917	.0000	.9127	.5238	.5166
.018	.9364	.3046	.0000	.9002	.5268	.5147
.016	.9278	.3548	.3224	.8859	.5026	.4823
.014	.9177	.4303	.4240	.8698	.4647	.4237
.012	.9040	.4884	.4776	.8524	.4313	.3478
.010	.8868	.4833	.4614	.8325	.4073	.2290
.008	.8566	.4316	.3409	.7923	.3818	.0000
.006	.8174	.3915	.0000	.7330	.3600	.0000
.004	.7527	.3626	.0000	.6455	.3414	.0000
			$Y = 0.23$			
.020	.9488	.2589	.0000	.9219	.4981	.4952
.018	.9425	.2690	.0000	.9097	.5279	.5234
.016	.9352	.2856	.2085	.8953	.5171	.5071
.014	.9258	.3872	.3814	.8786	.4853	.4634
.012	.9129	.4716	.4705	.8592	.4382	.3992
.010	.8953	.4992	.4883	.8380	.3942	.3094
.008	.8641	.4350	.3943	.8005	.3601	.0000
.006	.8238	.3778	.1913	.7404	.3439	.0000
.004	.7616	.3411	.0000	.6546	.3220	.0000

with the blue loops, the position of the circles becomes cooler and fainter as Z increases, which means that the envelope convection zone vanishes differently in the models with different Z. This is because the lower Z results in the lower opacity in the stellar envelope, too.

4. Properties of blue loops in low-Z and high-Z models

Our stellar models may develop the blue loops when Z is low or high enough, so we separate them into two kinds divided by $Z = 0.012$, around which η_c reaches the largest value in Table 1. This value of Z depends on the stellar mass, metallicity, etc., and our choice is in agreement with the results of BY27, AX70 and Dominguez (1999). A typical low-Z model is chosen to be one of $Z = 0.004$ and a typical high-Z model is one of $Z = 0.02$. By comparing the properties of the low-Z and high-Z models we may find how Z affects the blue loop.

From Fig. 4 we find that the energy generation of the central He core grows monotonically and that of the H-burning shell experiences a sudden increase during the early blue loop phase, which corresponds to the luminosity increase of the blue loop evolution. This result confirms that the luminosity variation of the blue loop comes from the nuclear energy in the H-burning shell for both low-Z and high-Z models. It should be pointed out that the position of the circle, which marks the disappearance of the envelope convection, is always located at the early ascending branch of the H-shell nuclear energy evolution in both CNO and CN models with the blue loops. The low-Z models usually have steep ascending branches of the H-shell nuclear energy production, and the rapid increase of the H-shell energy production makes the envelope contracting rapidly to increase the temperature and thermal conductivity coefficient, thus the envelope convection decreases rapidly. The rapid increase of the H-shell energy production in our models is not caused by the so-called secular instability, because the estimated thermal time-scale is much shorter than the time

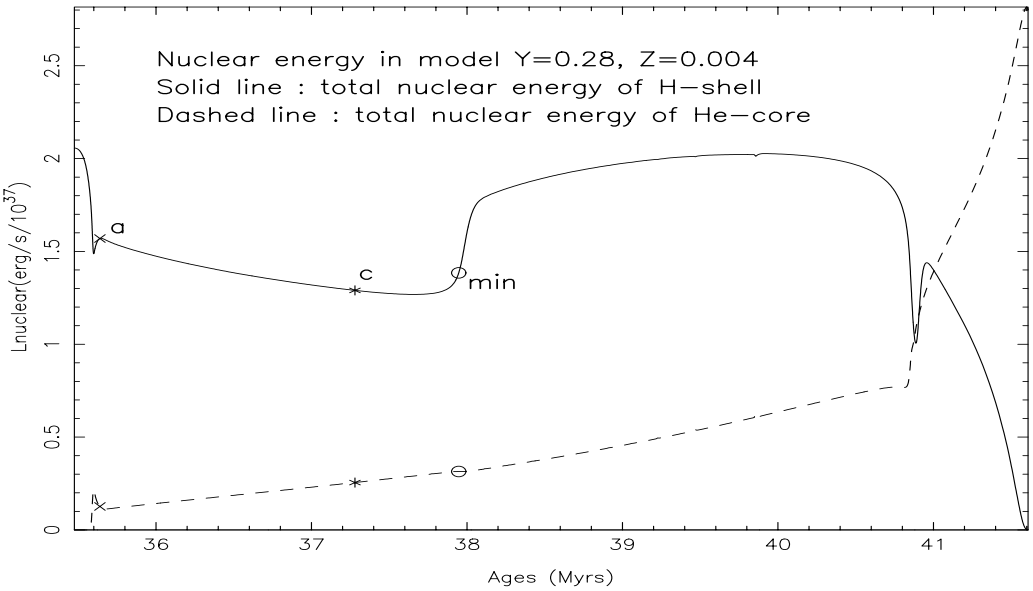

Fig. 4. The nuclear energy generated in the He-core (dashed) and the H-shell(solid) of the CNO model. The position of a, c, and min are marked by the same symbols as in Fig. 3.

considered, and more than 99% of the whole luminosity is contributed by the nuclear energy.

The nuclear energy variation in the H-burning shell is different between the low-Z model and the high-Z model. In the low-Z model, the energy production in the H-burning shell increases steeply in a short time and afterwards stays at a roughly steady high level for a long time. In the high-Z model, however, the H-shell energy production increases gradually with a moderate slope in the whole ascending branch of the blue loop.

The H-shell during the energy increase phase varies in a similar way in the high-Z and low-Z models from Fig. 5. The central temperature of the H-shell increases during this period, and this results from the envelope contraction and controls the nuclear energy production in the H-shell. The density and pressure of the H-shell decrease correspondingly, because the H-shell will expand and step out toward lower density and pressure regions. There are also some differences between these two models in Fig. 5. At the time of the minimum luminosity, the central temperature of the H-shell in the $Z = 0.004$ model is about 6% higher than that in the $Z = 0.02$ model, and the pressure is 9% larger. There is a steep decrease phase in the pressure and density, which corresponds to the sharp increase of the H-shell energy production in Fig. 4.

The central status of the low-Z model is quite different from that of the high-Z model in Fig. 6. Except for a short reverse period, the central density and pressure decrease in the low-Z model while increase in the high-Z model. On the other hand, the central temperature increases during the blue loop phase in both kinds of models. This difference may come from the fact that the blue loop evolution takes place in different stages of the central He-burning process in the low-Z and high-Z models (Kippenhahn & Weigert 1990 and references therein). During the early stage of the central He-burning process, the He-burning core expands slowly and the central density and pressure decrease correspondingly. Our low-Z model is in this stage when it develops the blue loop, because the central He abundance is as high as 0.633 at the beginning of the blue loop. When the helium abundance is low enough during the late stage of the central He burning, the stellar core has to contract to maintain the stellar luminosity still increasing and therefore to increase the pressure and density. Our high-Z model is in this phase and its central helium abundance is only 0.257 at the beginning of the blue loop.

The rapid variation of the H-shell in the model of $Z = 0.004$ can affect the stellar core structure from Figs. 5 and 6. It can be seen that the nuclear energy generation of the He core is suppressed when the H-shell burning increases rapidly. We ascribe this effect to the variation of the convective core. During the early stage of the central He burning, the convective core is usually larger than the central nuclear reaction region and expands slowly, therefore convection can bring fresh helium into the nuclear burning region. But when the H-burning shell is enlarging its nuclear energy production rapidly, the layer below the H-shell is heated and the core convection zone stops moving outward or even moves inward. So the nuclear burning core cannot get fresh helium anymore, and the He-burning core must contract to raise its pressure and density to maintain the steady state. This result indicates that the state of the He-core is not completely independent of the H-shell. In most stages of the central He burning process, however, the stellar core is indeed not disturbed by the envelope and H-shell, so we can take it as a good approximation in most cases. These differences between the models of $Z = 0.004$ and $Z = 0.02$ indicate that the low-Z and high-Z models develop their blue loops in different ways. The two models reach small η_c in different processes, and we will investigate this in the next section.

5. Effects of metallicity on blue loops

We have noticed that the metal abundance Z has two main effects on the blue loop. For low-Z models, lower opacities due

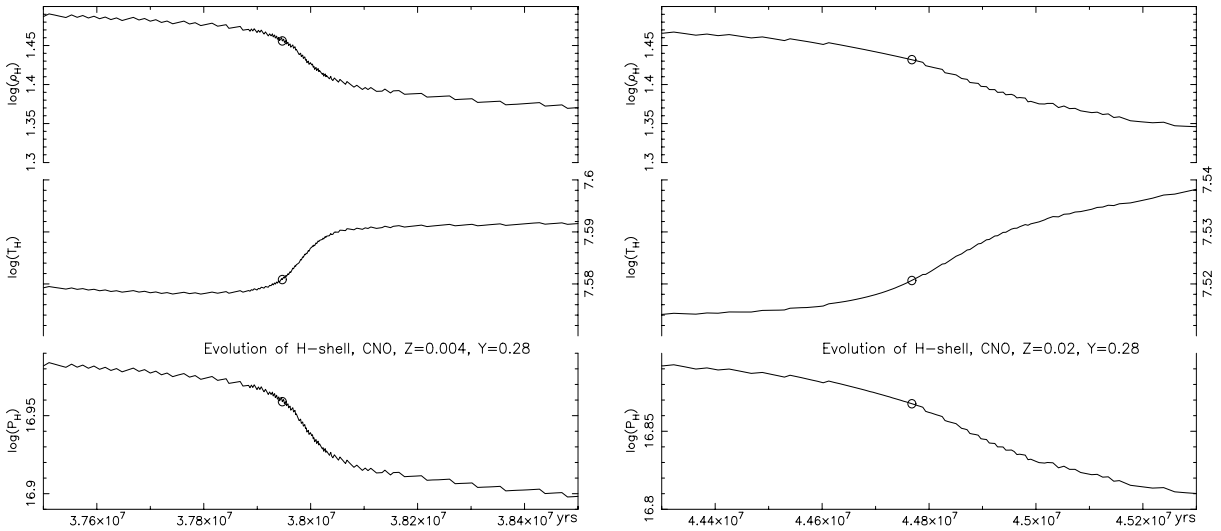

Fig. 5. Evolution of the H-shell near the min moment.

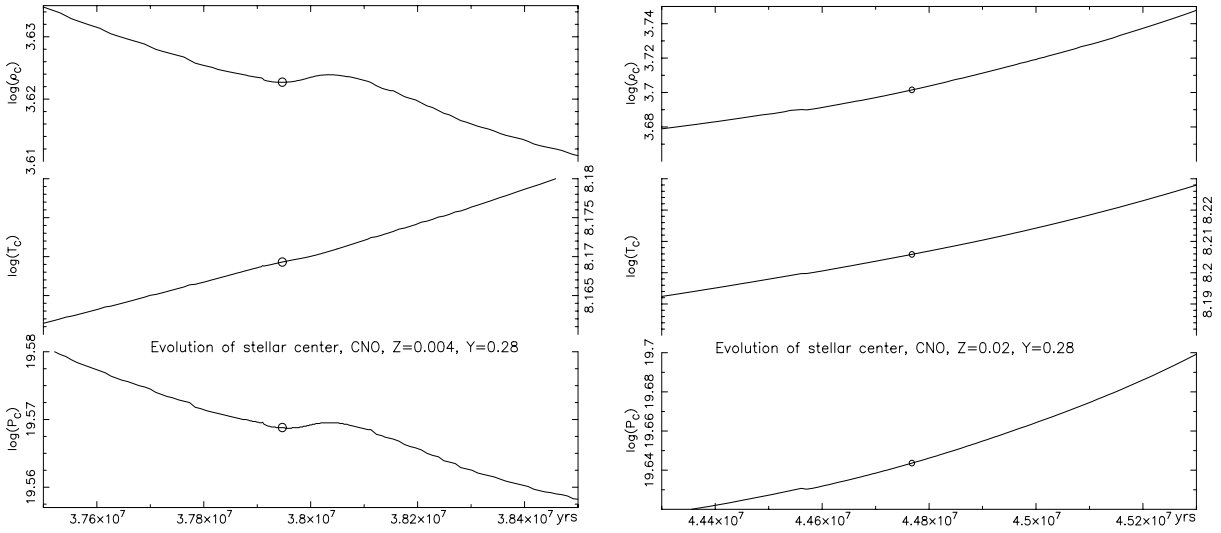

Fig. 6. Evolution of the stellar center near the min moment.

to lower Z facilitates the development of the blue loop according to many previous investigations (Stothers & Chin 1968; Castellani et al. 1990; Alongi et al. 1991; Schaller et al. 1992; Bono et al. 2000). Our results show that lower opacity in the stellar envelope makes the top of the RGB bluer, which leads to a smaller η_a as the envelope convection cannot penetrate inward so deeply. It is very important that a small η_a can strongly depress the development of the envelope convection, and the star will rapidly evolve to the bottom of the RGB with a fairly small η_c. Just like the mechanism we have discussed in Paper I, the envelope will contract rapidly and the star will develop an extended blue loop when η_c is smaller than the critical value. For high-Z models, higher ^{14}N abundance due to higher Z in the H-burning shell makes the H-shell burning more efficient and the "push effect" more effective, and the stellar envelop can therefore reach a larger η_a at the top of the RGB and a chemical discontinuity closer to the shell source, and a smaller η_c at the bottom of the RGB in the subsequent evolution, as we have already discussed in Paper I.

Taking account of these two effects of metallicity, we can explain the effects of Z on the blue loop according to Fig. 7. Along with the increase of Z from 0.004 to about 0.012, the envelope opacity increases to make η_c increase also. This postpones the formation of the blue loop and the width of the blue loop decreases, and furthermore the blue loop is eventually forbidden. These processes are all dominated by the envelope opacity, so that η_{min} increases whether it is a CNO or a CN model. With further increase of Z, the ^{14}N abundance in the CNO models takes effect and the two kinds of models evolve in different ways. For the CNO models in Fig. 7, when Z increases to 0.012 and X_N in the H-shell reaches about 0.008, the ^{14}N abundance in the H-shell is so high that it makes the "push effect" strong enough and η_{min} decreases gradually to zero, then the blue loop is rebuilt. We can find a critical value of X_N, about 0.008 when $Z = 0.012$, above which the blue loop will be reformed. For the CN models, however, the ^{14}N abundance of the H shell source is very low and cannot take effect for the considered values of Z. Under the control of increasing

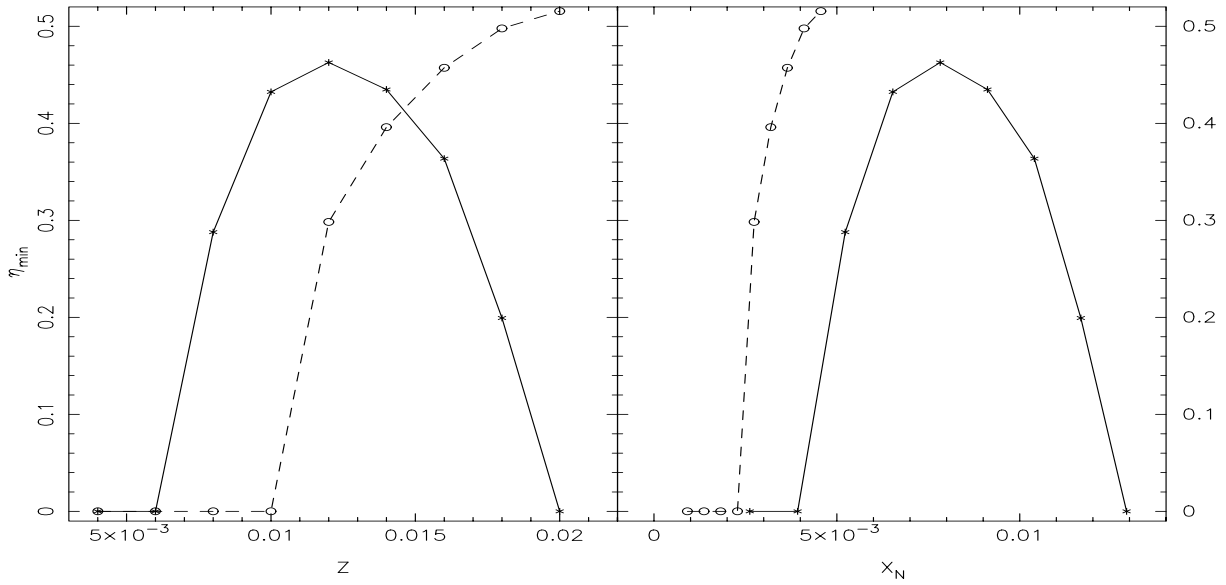

Fig. 7. $\eta_{\min}$ in the considered models ($Y = 0.28$) are plotted against the initial abundance Z and $X_{\rm N}$. The CNO (solid) and CN models (dashed) are plotted.

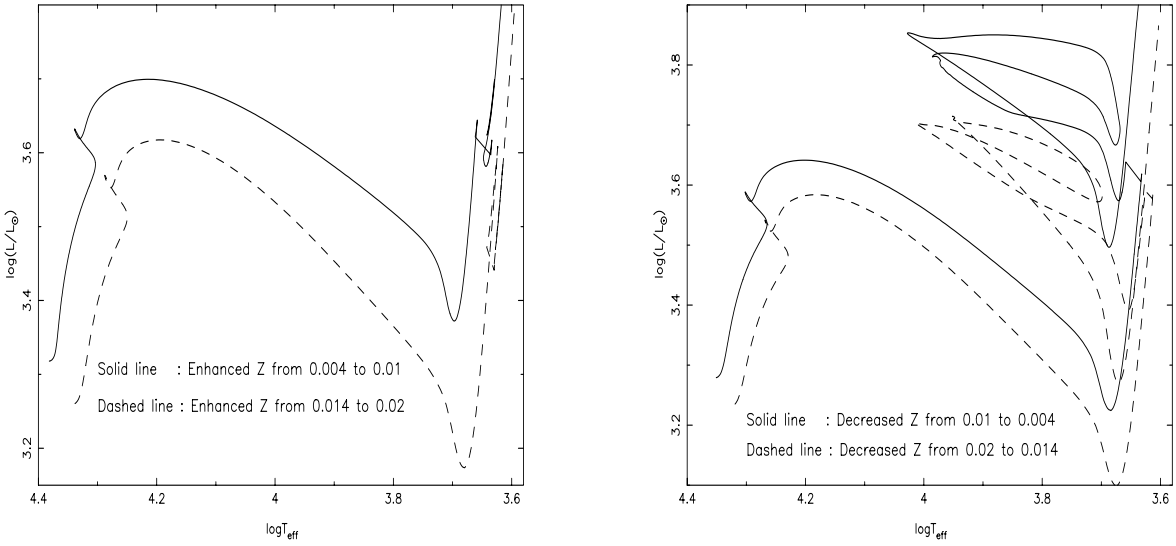

Fig. 8. Two kinds of models in which the envelope Z is enhanced (*left panel*) or decreased (*right panel*).

envelope opacity, $\eta_{\min}$ increases within the considered parameter range. Figure 7 shows that $\eta_{\min}$ of the CN models can become larger than 0.5 while $\eta_{\min}$ of the CNO models only get to about 0.46.

We verify the two effects of Z on the formation of the blue loop in Fig. 8. Two kinds of models are constructed, one is the enhanced-Z model and the other is the decreased-Z model. In the left panel, the metallicity in the stellar envelope is artificially increased from 0.004 to 0.01 for one model and from 0.014 to 0.02 for the other. The moment of this treatment is arranged just after the stars ignite their central helium burning (also the moment when the envelope convection zone is penetrating most), and the contaminated region is set in the stellar envelope beyond the hydrogen profile, to keep the X-profile unchanged. The solid line shows that the blue loop is forbidden and the star evolves like the model of $Z = 0.01$, and we can conclude that the contaminating process to increase the opacity of the envelope affects the evolution of the star. The dashed line shows that the blue loop is not developed and the star evolves like the model of $Z = 0.014$, and the contaminating process has no effect because the ^{14}N abundance in the H-shell is not enlarged to form the blue loop. In the right panel, the two opposite models with decreasing Z process in the stellar envelope also show that the star behaves like the model of $Z = 0.004$ when its envelope Z decreases from 0.01 to 0.004, and the other star evolves like the model of $Z = 0.02$ when its envelope Z decreases from 0.02 to 0.014. All of these models indicate that when Z is lower than about 0.012, the envelop Z dominates the evolution of the star, and when Z is higher than 0.012, the ^{14}N abundance in the H-shell dominates the behavior of the star.

6. Discussions and conclusions

By comparing the properties of low-Z and high-Z models, we have explored the effects of metallicity on the blue loop and put our focus on the formation of the blue loop in low-Z models. It has been found that lower opacities due to lower Z in the stellar envelope plays a crucial role in the formation of the blue loop. Although the star with lower opacity has a larger nuclear burning core and therefore a brighter luminosity at the top of the RGB, it has a hotter envelope and a bluer RGB, which effectively depresses the development of convection in the stellar envelope. When the envelope opacity is low enough, the stellar envelope will be radiation-dominated at the bottom of the RGB and its envelope convective ratio η_c, defined as the envelope convection mass divided by the total envelope mass, will be smaller than a critical value η_{crit}, and the star will form a blue loop in its subsequent evolution.

Comparing the high-Z and low-Z models, we have found that the formation mechanisms of the blue loops are different from each other. For low-Z models, lower metallicity makes the envelope opacity lower, which results in smaller η_a at the top of the RGB and thereafter smaller η_c at the bottom of the RGB. For high-Z models, higher Z results in higher ^{14}N abundance and more effective nuclear burning in the H-shell, which leads to two main effects. One is a larger η_a to let the envelope convection penetrate deeper and to leave an X-profile closer to the shell source. The other is a stronger "push effect" to let η_a rapidly decrease to smaller η_c along the descent of the RGB. A blue loop will be developed when η_c is lower than a critical value η_{crit}. Besides, we have found that the low-Z models form their blue loops in the early stage of the central helium burning, while the high-Z models form their blue loops in the late stage of the central helium burning. This has been identified by comparing the response of the stellar core to the rapid increase of the stellar luminosity during the beginning of the blue loop.

By comparing the blue loop evolution under different parameters, we have found that η_{crit} depends not only on the stellar mass (see Paper I), but also on the metallicity. From our numerical results, η_{crit} increases as Z decreases, which indicates that low-Z models form blue loops more easily. η_{crit} has been found to have a weak dependence on the initial helium abundance, and η_{crit} increases with Y. It should be noticed that the dependence of η_{crit} on the stellar mass, metallicity, and the initial helium may be different for high-Z and low-Z models, since the formation mechanisms of their blue loops are different.

We have confirmed that the envelope convective ratio at the bottom of the RGB, η_c, is an essential factor to determine whether a star develops a blue loop or not. The stellar models with very low or high metallicity are found to develop blue loops when η_c is lower than a critical value η_{crit}. This fact confirms the validity of η_c as a general criterion to determine the formation of a blue loop, as soon as the dependence of η_{crit} on the stellar mass, metallicity, and the initial helium abundance is established. η_c measures the physical structure of a stellar envelope just before the blue loop phase, and it cannot be a result of the blue loop evolution. When η_c is small enough, the stellar envelope is radiation-dominated. Under this condition and the constraint of the virial theorem, the only response of the stellar envelope to an increase of the stellar luminosity is to contract and to increase its thermal conductivity coefficient, to transfer the extra heat flowing through it.

It should be noticed that η_{crit} may depend on more physical ingredients, such as the mass loss through the stellar wind and between the binary system, overshooting from the convective core, element diffusion, etc., but the basic physics of the formation of the blue loop will not be changed. It can be applied to more complicated situations to analyze the formation of the blue loop.

Acknowledgements. This work is co-sponsored by the NSFC of China through grant number 19833040 and 10173024, National Key Fundamental Research Project through grant G1999075405 and G2000078401. The authors thank the anonymous referee for suggesting to pay attention to the differences of the triggering of the blue loop between low-Z and high-Z models. We thank R. Q. Huang, S. L. Bi, J. Y. Yang, and J. H. Guo for helpful discussions.

References

Alcock, C., & Paczynski, B. 1978, ApJ, 223, 244 (AX70)
Alexander, D. R., & Ferguson, J. W. 1994, ApJ, 437, 879
Alongi, M., Bertelli, G., Bressan, A., & Chiosi, C. 1991, A&A, 244, 95
Anders, E., & Grevesse, N. 1989, Geochim. Cosmochim. Acta, 53, 197
Bono, G., Caputo, F., Cassisi, S., et al. 2000, ApJ, 543, 955 (BY27)
Castellani, V., Chieffi, A., & Straniero, O. 1990, ApJS, 74, 463
Caughlan, G. R., & Fowler, W. A. 1988, Atomic Data and Nuclear Data Tables, 40, 283
Clayton, D. D. 1968, Principles of Stellar Evolution and Nucleosynthesis (US: McGraw-Hill Inc.)
Cox, J. P., & Giuli, R. T. 1968, Principles of Stellar Structure (New York: Gordon and Breach)
Dominguez, I., Chieffi, A., Limongi, M., & Straniero, O. 1999, ApJ, 524, 226
Fricke, K. J., & Strittmatter, P. A. 1972, MNRAS, 156, 129
Grevesse, N., & Noels, A. 1993, in Origin and Evolution of the Elements, ed. N. Prantzos, E. Vangioni, & M. Cassé (Cambridge: Cambridge Univ. Press), 15
Hallgren, E. L., & Cox, J. P. 1970, ApJ, 162, 993
Harris, G. L., & Deupree, R. 1976, ApJ, 209, 402
Hofmeister, E. 1967, Z. Astrophys., 65, 164
Huang, R. Q., & Yu, K. N. 1998, Stellar Astrophysics (Singapore: Springer-Verlag)
Iglesias, C. A., & Rogers, F. J. 1996, ApJ, 464, 943
Kippenhahn, R., Weigert, A., & Hofmeister, E. 1967, Methods in Computational Physics, 7 (New York: Academic Press), 129
Kippenhahn, R., & Weigert, A. 1990, Stellar Structure and Evolution (Berlin: Springer)
Pols, O. R., Schroder, K. P., Hurley, J. R., Tout, C. A., & Eggleton, P. P. 1998, MNRAS, 298, 525
Renzini, A., Greggio, L., & Ritossa, C. 1992, ApJ, 400, 280
Robertson, J. W. 1971, ApJ, 170, 353
Robertson, J. W. 1972a, ApJ, 173, 631
Robertson, J. W. 1972b, ApJ, 177, 473
Schaller., G., Schaerer, D., Meynet, G., & Maeder, A. 1992, A&AS, 96, 269
Schlesinger, B. M. 1969, ApJ, 158, 1059
Schlesinger, B. M. 1977, ApJ, 212, 507
Stothers, R. B., & Chin, C. W. 1968, ApJ, 152, 225
Stothers, R. B., & Chin, C. W. 1973, ApJ, 175, 555
Stothers, R. B., & Chin, C. W. 1991, ApJ, 374, 288
Xu, H. Y., & Li, Y. 2004, A&A, 418, 213 (Paper I)